

OPTIMAL FILTERING APPLIED TO THE VACUUM ARC REMELTING PROCESS

Rodney L. Williamson,[†] Joseph J. Beaman[‡] and David K. Melgaard[†]

[†]Liquid Metals Processing Lab
Sandia National Laboratories
Albuquerque, New Mexico 87185-1134

[‡]Mechanical Engineering Department
University of Texas
Austin, Texas 78712

Abstract

Optimal estimation theory has been applied to the problem of estimating process variables during vacuum arc remelting (VAR), a process widely used in the specialty metals industry to cast large ingots of segregation sensitive and/or reactive metal alloys. Four state variables were used to develop a simple state-space model of the VAR process: electrode gap (G), electrode mass (M), electrode position (X) and electrode melting rate (R). The optimal estimator consists of a Kalman filter that incorporates the model and uses electrode feed rate and measurement based estimates of G, M and X to produce optimal estimates of all four state variables. Simulations show that the filter provides estimates that have error variances between one and three orders-of-magnitude less than estimates based solely on measurements. Examples are presented that verify this for electrode gap, an extremely important control parameter for the process.

DISCLAIMER

This report was prepared as an account of work sponsored by an agency of the United States Government. Neither the United States Government nor any agency thereof, nor any of their employees, make any warranty, express or implied, or assumes any legal liability or responsibility for the accuracy, completeness, or usefulness of any information, apparatus, product, or process disclosed, or represents that its use would not infringe privately owned rights. Reference herein to any specific commercial product, process, or service by trade name, trademark, manufacturer, or otherwise does not necessarily constitute or imply its endorsement, recommendation, or favoring by the United States Government or any agency thereof. The views and opinions of authors expressed herein do not necessarily state or reflect those of the United States Government or any agency thereof.

DISCLAIMER

**Portions of this document may be illegible
in electronic image products. Images are
produced from the best available original
document.**

Introduction

Vacuum arc remelting (VAR) is a process used throughout the specialty metals industry for controlled casting of segregation sensitive and reactive metal alloy ingots. Of particular importance in the former group are nickel-base superalloys, whereas common reactive metal alloys include titanium and zirconium alloys. In this process, a cylindrically shaped, alloy electrode is loaded into the water-cooled, copper crucible of a VAR furnace, the furnace is evacuated, and a DC arc is struck between the electrode (cathode) and some start material (e.g. metal chips) at the bottom of the crucible (anode). The arc heats both the start material and the electrode tip, eventually melting both. As the electrode tip is melted away, molten metal drips off and an ingot forms in the copper crucible. Because the crucible diameter is typically 0.05-0.15 m larger than the electrode diameter, the electrode must be translated downward toward the anode pool to keep the mean distance between the electrode tip and pool surface constant. This mean distance is called the electrode gap. The objective of VAR is to produce an ingot of appropriate grain structure that is free of segregation, porosity, shrinkage cavities, or any other defects associated with uncontrolled solidification during casting. A schematic depiction of the VAR process is presented in Figure 1.

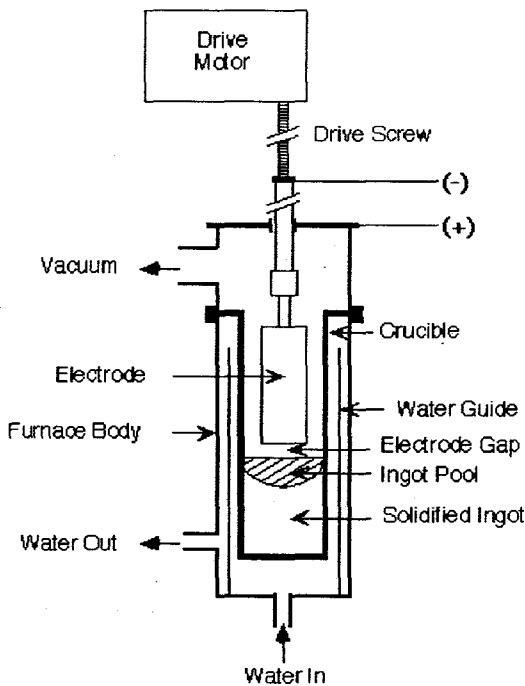


Figure 1. A schematic diagram of a VAR furnace.

In industrial practice, several process variables are monitored and recorded to track the progress and evaluate the status of the VAR process. These include arc voltage, melting current, electrode position, and electrode mass. Additionally, during VAR of premium grade superalloys, drip-short frequency is added to this list. A drip-short occurs when a molten metal droplet hanging down from the electrode tip contacts the surface of the molten pool atop the ingot thereby causing a momentary interruption of the arc.¹ The frequency of these events can be related to the magnitude of the electrode gap.² Electrode gap can also be estimated from the magnitude of the mean arc voltage.³

Accurate estimation of electrode gap is critical to successfully carrying out the VAR process. Variations in this parameter can cause defects to form in the ingot.⁴ Unfortunately, electrode

gap estimates based on arc voltage and drip-short frequency are very noisy and averaging over tens of seconds is required to obtain sufficiently accurate information. Melt rate estimates based on electrode weight measurements are worse still. It is common practice in many industrial melt shops to estimate melt rate from the slope of a twenty minute sliding window of electrode mass data.

The problem of noisy estimates directly impacts the problem of process control. Commanded electrode velocity is dependent on average drip-short frequency or arc voltage for feedback. This makes for a highly damped electrode drive system that is unable to react to process transients and upsets in a timely fashion. Melt rate estimates are either so noisy or so highly damped that active current control using melt rate estimates for feedback is not practical. Common industrial practice requires that the melting current be controlled to a constant, steady-state value characteristic of a material and electrode/ingot size. Occasionally a shop will use measured melt rate to trim around the steady-state current.

This paper focuses on the development of a VAR process filter that facilitates acquiring accurate, instantaneous variable estimates for the purpose of process monitoring and electrode gap control. A dynamic model of electrode gap is developed and a discrete state-space model of the process is formed in terms of four state variables: electrode gap (G), electrode mass (M), electrode position (X), and electrode melting rate ($R = \dot{M}$). The single input to the system is electrode drive velocity, \dot{X} , written as V below. An optimal estimator is then developed using Kalman filter theory. The performance of the filter is evaluated using simulations. Electrode gap data are presented from actual laboratory and industrial tests to verify the performance improvements predicted by the simulations.

Filter Development

The electrode gap dynamics are described by the following differential equation:

$$\dot{G} = \dot{l}_{el} - \dot{h}_{ing} - V. \quad (1)$$

This equation states that, over a vanishingly short time interval, the change in gap equals the change in electrode length (\dot{l}_{el}) due to melting less the change in ingot height (\dot{h}_{ing}) due to mold filling and the change in electrode position due to its being driven down. The first term on the right can be found by assuming that liquid metal leaves the surface as soon as it forms and that the electrode tip surface is flat with an area given by ϵA_e where A_e is the room temperature cross-sectional area and ϵ accounts for the effects of thermal expansion. The resulting expression is

$$\dot{l}_{el} = \frac{R}{\rho_{liq} \epsilon A_e} \quad (2)$$

where ρ_{liq} is the liquid metal alloy density.

The second term in Eq. (1) is directly related to the first since the ingot is formed from material melted off the electrode. The relationship is complicated by the fact that the ingot is being cooled and its density is a function of both ingot height and radial ingot position. In steady-state, it is assumed that the change in ingot height with time can be described by

$$h_{ing} = \kappa \frac{A_e}{A_i} i_{el} \quad (3)$$

where κ is a constant factor that corrects the room temperature electrode/ingot area ratio (often called the fill ratio) for thermal effects. This is born out in practice where it is found that, under steady-state melting conditions, a linear drive speed is required to achieve a constant electrode gap.

Substituting Eq.'s (2) and (3) into Eq. (1) gives the following expression for the time dependent gap behavior:

$$\dot{G} = \frac{1}{\rho_{liq} \epsilon} \left(\frac{1}{A_e} - \frac{\kappa}{A_i} \right) R - V = \alpha R - V \quad (4)$$

In practice, an average value for α is estimated from melt data for a particular process.

Using the state-space formalism, the discrete time VAR process can be described by a matrix equation of the form

$$x_{n+1} = Ax_n + Bu_n + Nw_n \quad (5)$$

where A , B and N are the transition, input, and process noise matrices, respectively, x is the state vector consisting of the four variables listed in the Introduction, and u is the control input "vector" consisting only of the electrode drive speed. N operates on w , a vector characterizing the uncertainty in the inputs that drive the plant as well as uncertainty in the plant itself. These terms constitute the process noise. It is assumed that each component of w can be represented in discrete time by a white sequence with zero-mean. In other words, the process noise is uncorrelated and unbiased. The subscripts in Eq. (5) refer to time-steps in the discrete time system. A , B and N are determined by considering the dynamics of the VAR process.

As seen above, changes in electrode gap are directly related to the relative velocities of the growing ingot and moving, melting electrode. Converting Eq. (4) to discrete time and accounting for process uncertainty, the electrode gap dynamics are described by

$$G_{n+1} = G_n + \alpha R_n T - V_n T - w_{X_n(V)} + R_0 T w_{\alpha_n} \quad (6)$$

where T is the sample time, R_0 is the nominal melt rate, $w_{X_n(V)}$ quantifies the uncertainty in electrode position due to uncertainty in the electrode drive velocity, and w_{α_n} quantifies uncertainty in α . This uncertainty stems from surface variations in both the electrode and crucible, variation in the electrode cross-sectional area due to voids, and fluctuating temperature distributions in both the electrode and ingot.

The dynamics of the electrode mass are directly related to melt rate by

$$M_{n+1} = M_n - R_n T. \quad (7)$$

In words, the mass at t_{n+1} is the mass at t_n less what melted off in the time interval T .

Position changes are tied directly to velocity according to

$$X_{n+1} = X_n + V_n T + w X_n(V). \quad (8)$$

The position at t_{n+1} is just the position at t_n plus the distance moved in the last time step corrected for the uncertainty in the electrode drive velocity.

Finally, the formulation assumes that the melt rate is a random variable with no driving term so that the dynamics are simply described by

$$R_{n+1} = R_n + w R_n \quad (9)$$

where $w R_n$ quantifies the uncertainty in the melt rate. Note that Eq. (9) does not guarantee that the melt rate will remain indefinitely at its initial value. Indeed, over a time period consisting of many time steps it will randomly walk away from that value, the maximum step size of the walk being determined by the uncertainty. In practice, the plant behavior differs from this because one attempts to drive the melt rate with melting current. Insofar as the development of the filter is concerned, this is irrelevant so long as one has correctly accounted for the process and measurement noise sources.⁵

The development has assumed a straight electrode and crucible: A_e and A_i are not functions of time. However, it is often the case that melting is performed with both tapered electrode and crucible for the simple reason that a tapered casting is easier to remove from the mold. Because of this, it is not uncommon for α to vary linearly by 10-20% over the duration of a VAR melt. One may easily account for this non-random error by modeling the time-dependent behavior of α , an exercise that adds complication to the filter development but nothing conceptually to the way it works and performs. For this reason, the more complicated formulation is not given here. However, a simple method of including this feature in the model is to linearize Eq. (4) about the nominal values (α_0, R_0, V_0), and then add a new state variable $\Delta\alpha = \alpha - \alpha_0$ where α is now a function of the amount of material melted.

Making appropriate substitutions, Eq. (5) can be written as

$$\begin{bmatrix} G_{n+1} \\ M_{n+1} \\ X_{n+1} \\ R_{n+1} \end{bmatrix} = A \begin{bmatrix} G_n \\ M_n \\ X_n \\ R_n \end{bmatrix} + B[V_n] + N \begin{bmatrix} w X_n(V) \\ w \alpha_n \\ w R_n \end{bmatrix}. \quad (10)$$

which relates the electrode gap, mass, position and melt rate at t_{n+1} to their values at t_n given both deterministic and random inputs. A, B and N can now be derived from inspection of Eq.'s (6)-(10). They are

$$A = \begin{bmatrix} 1 & 0 & 0 & \alpha T \\ 0 & 1 & 0 & -T \\ 0 & 0 & 1 & 0 \\ 0 & 0 & 0 & 1 \end{bmatrix} \quad (11)$$

$$B = \begin{bmatrix} -T \\ 0 \\ T \\ 0 \end{bmatrix} \quad (12)$$

and

$$N = \begin{bmatrix} -1 & R_0 T & 0 \\ 0 & 0 & 0 \\ 1 & 0 & 0 \\ 0 & 0 & 1 \end{bmatrix} \quad (13)$$

Besides state variables and inputs, the system is also characterized by outputs, some, or all, of which can be measured. The outputs for this system are taken to be electrode gap, mass and position. The output equation is then given by

$$\begin{bmatrix} G_n \\ M_n \\ X_n \end{bmatrix} = C \begin{bmatrix} G_n \\ M_n \\ X_n \\ R_n \end{bmatrix} \quad (14)$$

Again by inspection, it is seen the C must be given by

$$C = \begin{bmatrix} 1 & 0 & 0 & 0 \\ 0 & 1 & 0 & 0 \\ 0 & 0 & 1 & 0 \end{bmatrix} \quad (15)$$

Assuming that all outputs can be measured, the measurements at t_n are modeled by

$$z_n = C \begin{bmatrix} G_n \\ M_n \\ X_n \\ R_n \end{bmatrix} + \begin{bmatrix} v_{G_n} \\ v_{M_n} \\ v_{X_n} \end{bmatrix} \quad (16)$$

where the elements of the column vector, v_n , characterize the measurement noise (assumed white with zero mean) present in the gap, mass and position measurements.⁶

Given the process and measurement models embodied in Eq.'s (6)–(16), a Kalman filter (or optimal state observer) can be constructed using known methods the details of which are presented in standard texts on modern control system design.⁷ The equation for the filter in discrete time is

$$\hat{x}_{n+1} = A\hat{x}_n + Bu_n + M_K(z_n - C\hat{x}_n) \quad (17)$$

where A, B and C are as defined above for the plant, and a "hat" over a variable denotes an estimate. \hat{x}_{n+1} is the predicted system state at t_{n+1} estimated from measurements and the estimated state at t_n . The Kalman matrix, M_K , is chosen so as to minimize the error covariance of the estimated variables relative to their true values and can be derived from the steady-state process and measurement noise covariances. There are as many columns in M_K as measured system outputs, and as many rows as state variables. In the present application, M_K is a 4x3 matrix. Off-diagonal elements arise because of couplings between the variables. For example, \hat{G} is related to the measured values of all three outputs since $w_{X_n}(V)$ is a position term and melt rate is directly related to electrode mass (Eq. (6)). Therefore, the first row of M_K contains all non-zero values. On the other hand, there is no measurement for α and, thus, no corresponding element in M_K . The difference term in Eq. (17), called the innovation, goes to zero only in the case where the measurements are noise free and match perfectly the model predictions. In this situation, the future state is perfectly predicted from the present state by the system model, and all estimated values exactly equal the actual values. This situation never holds in practice.

The Kalman filter produces estimates of the future state and current outputs. These estimates are tied to process and measurement noise through a model of the system according to an optimal weighting scheme. If the process inputs and parameters are known with a high degree of precision relative to the measured outputs, the estimates will not be greatly influenced by the measurements, i.e. the filter "knows" that the measurements cannot be trusted. In this case, the elements of M_K will be very small and the estimator will be model based. The filter simply takes advantage of the fact that the state of the system is nearly completely determined by the physical constraints placed on it by the inputs and process variables coupled with knowledge of the previous state. On the other hand, if relatively exact measurements are available, the estimator will weigh them more heavily than the process model and the filter will be measurement based. Obviously, if all the outputs can be measured exactly, they do not need to be estimated.

Filter Performance

A block diagram of the VAR process model coupled to the Kalman filter is shown in Figure 2. A computer program was written using the Matlab™ programming language (The Math Works, Inc., Natick, MA) for the purpose of evaluating the improvement in the Kalman estimated outputs relative to the measured values. The simulations assume a 0.432 m (17 in.) diameter electrode being melted into 0.508 m (20 in.) diameter ingot at a nominal melt rate of 0.060 kg/s (476 lb/hr) and electrode drive speed of $\sim 1.8 \times 10^{-5}$ m/s (2.6 in./hr). These parameters are typical for VAR of Alloy 718. α is taken to be 2.94×10^{-4} m/kg based on experience melting this type and size material at this melt rate. This number is about 9% larger than what would be obtained by simply setting $\epsilon=\kappa=1$ in the expression for α . In the simulations, a sample time of 4 seconds was used.

The random sequences characterizing the process and measurement noise terms are each described by a standard deviation and variance. In practice these are determined through process characterization. For the simulations, $\sigma_{X(V)}$ was set to 2.0×10^{-6} m corresponding to an uncertainty in V of 5.0×10^{-7} m/s, and σ_R was set to 1.0×10^{-4} kg/s. σ_α was estimated to be about 5% of the nominal value, or 1.3×10^{-5} m/kg, by assuming that the electrode and crucible radii vary by only ± 0.001 m over the duration of the melt, that the density is known to within ± 100 kg/m³, and that the other parameters are constant. The measurement noise (standard deviation) terms were set to 5×10^{-3} m, 1 kg and 10^{-3} m for v_G , v_M and v_X , respectively. These are believed to be typical of the measurement capabilities available on many VAR furnaces in industry.

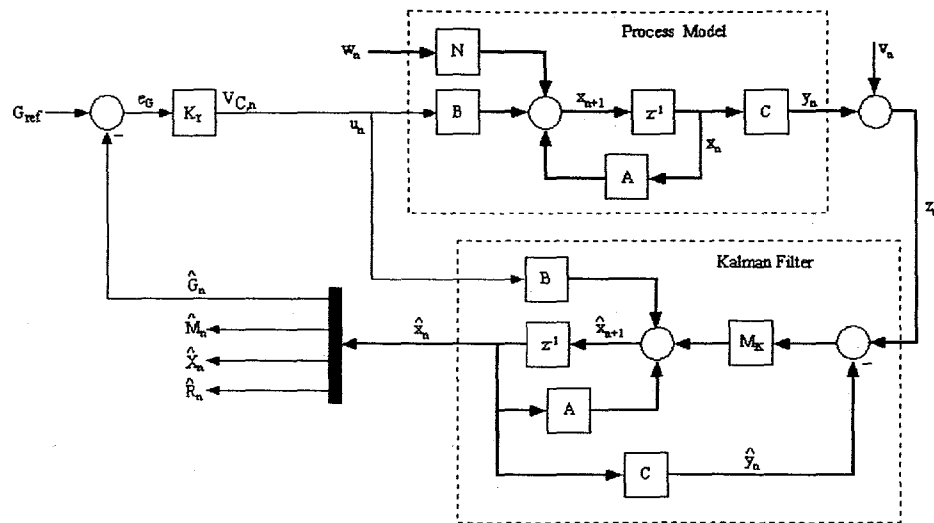


Figure 2. A block diagram showing the VAR process coupled to the Kalman filter. The Process Model replaces the actual plant in the simulations.

Figure 3 shows a plot of G and \hat{G} (its filtered value) resulting from a 5000 s simulation for an open-loop system (no feedback). V was set to 1.755×10^{-5} m/s in this simulation. The figure demonstrates that \hat{G} (G_e) tracks the “true” gap (G) very well. Drift in the gap from the nominal value of 0.01 m is due to the uncertainties in the system. Because of the random errors in the system, the difference between the gap and its nominal value follows a random walk trajectory.

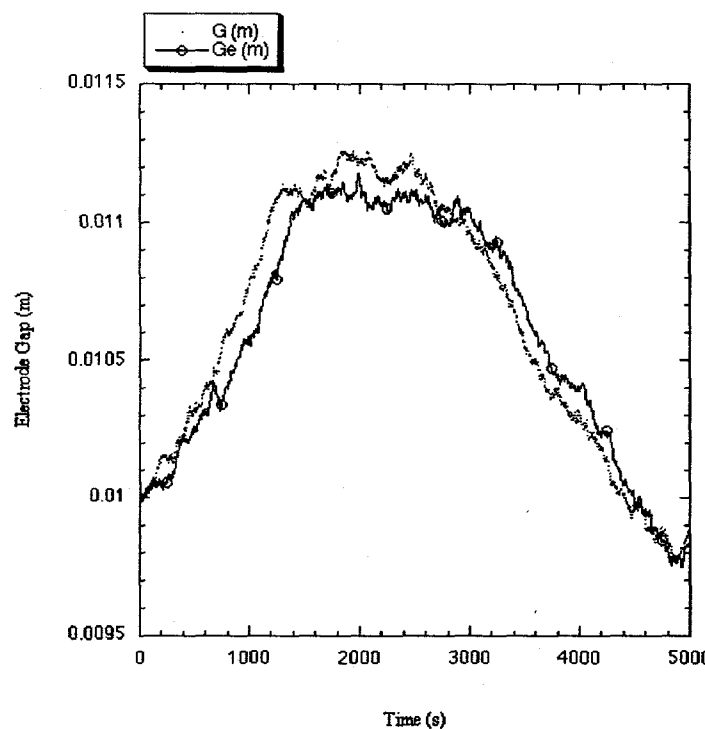


Figure 3. Simulated open-loop estimation of electrode gap.

\hat{G} is shown in Figure 4 plotted with the simulated measurement based estimate of electrode gap. The noise reduction achieved through Kalman filtering is readily apparent. This effect is seen in Table I, where error variances are tabulated for the measured and corresponding estimated outputs of the simulation. Note that the variances in the simulated measurements approximately equal the squares of the specified measurement noise terms, as required. Also note that the error variance in \hat{G} may change by as much as a factor of two from simulation to simulation whereas the error variances for the other estimates are more stable.

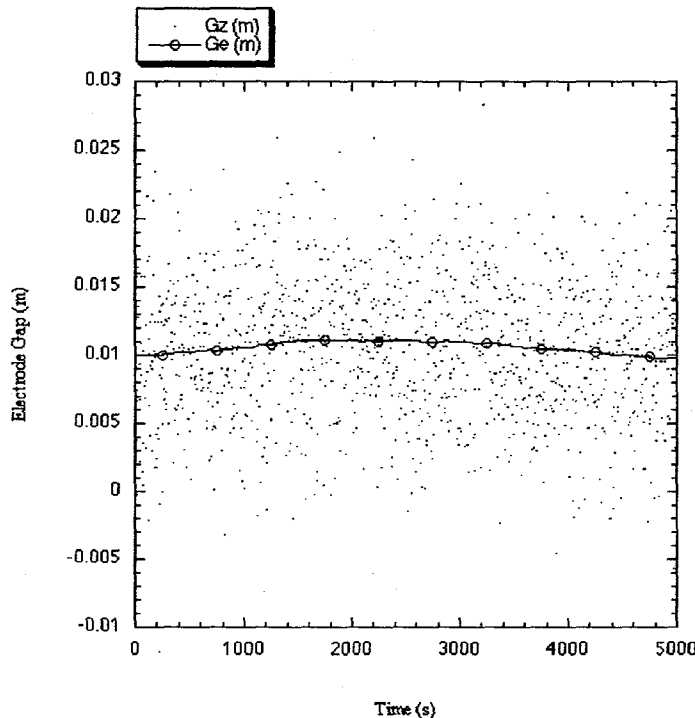


Figure 4. Simulated measured (G_z) and filtered (G_e) electrode gap.

Table I. Variances of measured (~) and filtered (^) variables.

$Var.(\tilde{G} - G)$	2.5×10^{-5}
$Var.(\hat{G} - G)$	1.3×10^{-8}
$Var.(\tilde{M} - M)$	0.99
$Var.(\hat{M} - M)$	2.5×10^{-2}
$Var.(\tilde{X} - X)$	9.7×10^{-7}
$Var.(\hat{X} - X)$	2.3×10^{-9}

Gap estimation was found to be sensitive to either increases or decreases in the gap measurement error indicating that the estimator, as defined, is neither completely model- nor measurement based. However, estimates are insensitive to measurement error once it has been increased beyond about ± 0.1 m, indicating that the estimator is model based under these measurement conditions. In other words, if one cannot measure gap to better than ± 0.1 m under these process conditions, the measurement is irrelevant to gap estimation. On the other hand, the estimator is completely measurement based with respect to gap measurement at a measurement resolution of $\pm 5 \times 10^{-6}$ m. At this resolution, the estimator becomes superfluous.

Simulation shows that accurate mass measurements (± 1 kg) are beneficial for electrode gap estimation. However, improvements beyond this have little effect. Increasing the measurement error adversely affects the gap estimate up to about ± 20 kg. Under the process conditions investigated, one might as well have no mass measurement at all if the error is increased beyond this value. Thus, with respect to electrode mass measurement, the estimator is model based beyond a measurement error of about ± 20 kg and measurement based at measurement errors less than ± 1 kg.

Simulation further indicates that gap estimation is not improved significantly by improving the resolution of the position measurement under the simulation conditions investigated. One must resist concluding from this that exact position measurements are of little intrinsic value to gap estimation. This depends on the uncertainties characterizing the system. For example, if one has poor ram control, the error covariance in \hat{G} may be significantly reduced by increasing the position measurement resolution. In general, complete system characterization is required before one can decide how to improve the estimation of important process variables.

Verification of Simulation Results for Electrode Gap

The simulations were performed for hypothetical situations considered to be typical of actual VAR processes. It is appropriate to show some sample data to verify that significant reductions in the noise characteristics of parameter estimates can be realized in actual practice by using Kalman filtering. As pointed out in the introduction, accurate electrode gap estimation is necessary for successful control of the VAR process. Electrode gap data from two test melts are shown below. Each example includes measurement based and Kalman filtered estimates of electrode gap. It should be noted that the filters used in the two examples differ in their details from the one developed above. This is because the tests involved estimation of additional control variables important for controlling aspects of the process not discussed in this paper. Information concerning these tests and the estimators they employed is unavailable for publication at this time. However, the dynamics described by Eq.'s (6)–(9) are captured in these more general filters and the examples are appropriate to illustrate the improvements in noise reduction realized by Kalman filtering.

The data shown in Figure 5 were acquired during VAR of 0.203 m diameter Alloy 718 electrode into 0.254 m diameter ingot on the VAR furnace at Sandia National Laboratories. Neither the electrode nor the crucible were tapered. Because there is no mass transducer (load cell) on this furnace, the measurement uncertainty is infinite for electrode mass. Melt rate derived from position measurements during the interval shown was estimated to be 0.040 ± 0.002 kg/s and the drive speed noise was similar to that used for the simulations. A high resolution encoder is mounted on the furnace so that the resolution in X was 10^{-5} m. The noise variance in the drip-short based measurement of G was 2.6×10^{-5} m². In comparison, the variance in the Kalman filter estimate of G was 5.1×10^{-9} m² giving a signal to noise improvement of about 70. Drive speed control decisions were made every two seconds based on the filtered estimates. The

controller was stable at very tight gaps (0.006 m). Intrusive gap measurements accomplished by driving the ram down until a dead short was achieved demonstrated that the controller was accurate to within the measurement error (± 0.001 m).

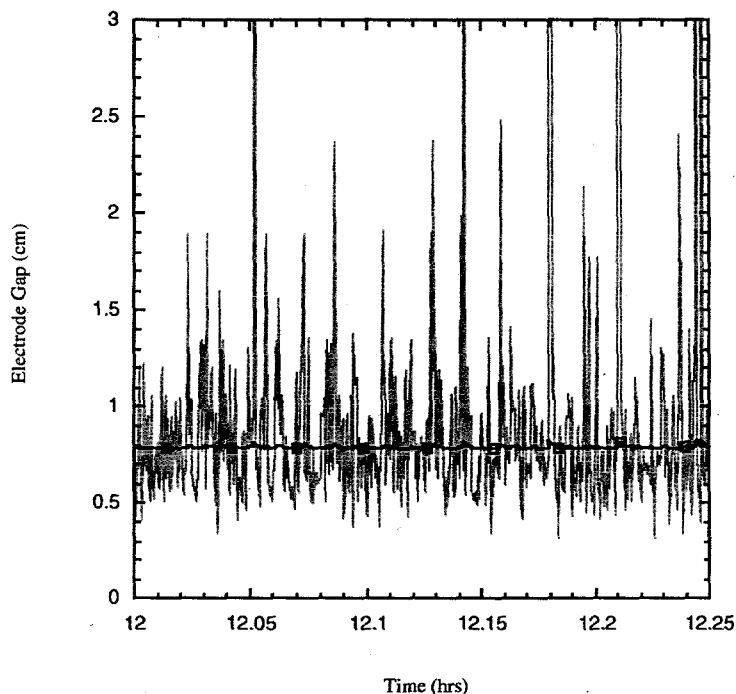


Figure 5. Plot of Kalman filtered gap estimate (solid w/squares) and estimates based on the measured drip short frequency.

The data shown in Figure 6 were acquired during VAR of Alloy 718 of the same size and under similar conditions to those for which the simulation was performed. Electrode gap was actively controlled during this melt based on feedback from the estimator. Two significant differences between the filter used for the simulation and the one used in the actual test melt must be noted. First, the filter was designed based on a load cell transducer uncertainty of ± 0.5 kg. Second, because of a problem with data transfer from the position transducer, electrode position measurements were not available for this test requiring an infinite position uncertainty to be used in the filter design. Even without the position measurement, the reduction in noise of the filtered gap estimates relative to those based on drip-short measurements is clearly significant. The sudden change at ~ 9.05 hours was the result of a commanded gap step from 0.012 m to 0.010 m.

Discussion

Optimal estimation techniques were originally developed for application in systems where measurements of key process variables are either very noisy or unavailable. Under such circumstances, a predictive process model can be incorporated into a process "observer" as depicted in Figure 2. Given the uncertainties in the measurements and model, the observer (Kalman filter) can produce estimates of the state variables of known uncertainty. If no measurement is available for a particular variable, the measurement uncertainty is set to infinity and the filter produces a purely model based estimate of the variable. It is natural to apply this

technology to estimating electrode gap in the VAR process where one encounters noisy measurements that are often spoiled by common process disturbances.

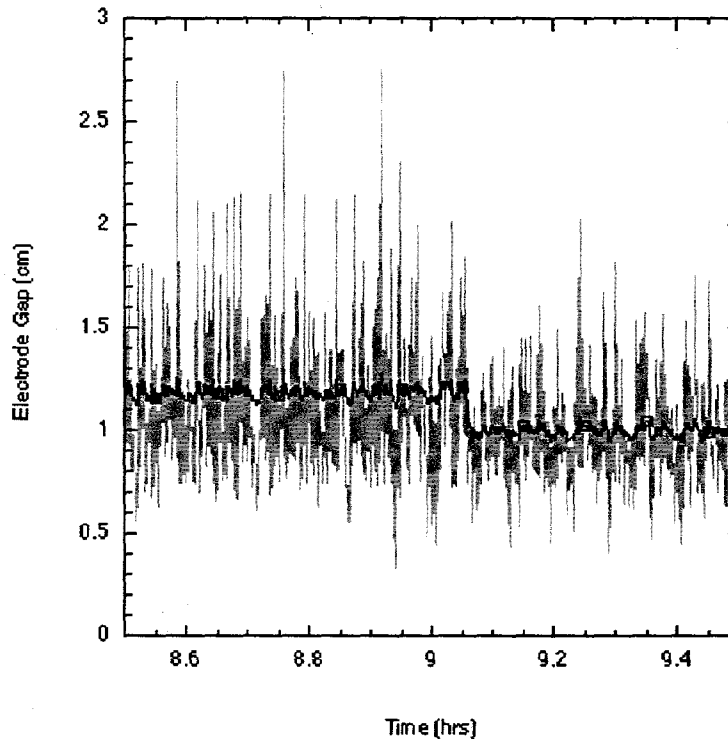


Figure 6. Plot of Kalman filtered gap estimate (solid w/squares) and estimates based on the measured drip short frequency.

Given the noise inherent in drip-short and arc voltage data, it is to be expected that estimates of electrode gap based on these data will be highly uncertain after only a few seconds of data acquisition. Often the uncertainty in the estimate exceeds the magnitude of the control reference. However, given the process inputs and noise characteristics, and the last state estimate, one can determine, based on physics alone, how much the gap could possibly have changed during the last time step. It is this physics based limitation that the filter imposes on the gap measurement and, for this reason, this type of filtering is sometimes called "physical filtering." Physical filtering constrains the estimate to be consistent with the physical situation as described by the model and the measurements. In the case of electrode gap, the filter requires that the estimated change from one time step to the next be consistent with the electrode velocity and melting rate as described by Eq. 6 as well as the measurement based estimation. The relative weights of the two estimates are reflected in the elements of the Kalman gain matrix and depend on the process and measurement uncertainties.

Though the focus of this paper has been electrode gap estimation, it has been made clear that the filter produces estimates of all state variables, including melt rate (Figure 2). Melt rate was not included as a measurement because of the difficulty involved with obtaining it from electrode mass measurements as mentioned in the Introduction. This difficulty arises because of the noise introduced into the measurement based estimate by taking the derivative of the mass transducer output. Determining the slope over long time intervals (10-20 minute) of mass data helps with the noise but introduces unacceptable lag into the estimate and effectively "erases" short term

transients. The simple filter developed for this paper effectively addresses this issue and its use in an actual system would, no doubt, result in a significant improvement in melt rate estimation. However, no experimental test involving this particular filter has been performed to confirm this. The latest generation of VAR controllers developed by Sandia National Laboratories and the Specialty Metals Process Consortium does, indeed, employ Kalman filtering to produce accurate, relatively noise-free melt rate estimates, but the filtering relies on a significantly more complex state-space model with respect to electrode melting dynamics. As a result, the melt rate estimate is affected by variables missing from Eq. (9) and the results are not germane to this study. This more advanced technology is described in a disclosure recently submitted to the United States Patent Office and further information related to it is not yet available for external publication.

Conclusions

The following conclusions can be made from this work:

1. Kalman filtering provides a superior means of estimating electrode gap for VAR process control. The estimates are significantly less noisy and provide the basis for improving both the stability and response of the control system.
2. The Kalman filter development described here provides a means of estimating electrode melting rate that is not dependent on differentiating the load cell output. Hence, the estimates are not heavily damped and are useful for electrode gap control purposes.
3. The error variance of the gap estimate could be affected by either increasing or decreasing the gap measurement uncertainty indicating that, under the process conditions of interest, the estimator was neither completely model based nor measurement based. Increasing the measurement error beyond ± 0.1 m is equivalent to having no gap measurement at all.
4. An accurate electrode mass measurement is beneficial for electrode gap control up to an accuracy of ± 1 kg under the process conditions investigated. Increasing the mass measurement error to ± 20 kg is tantamount to having no mass data at all.
5. Increasing or decreasing the position measurement error has little effect unless one has poor ram control. With poor ram control, accurate, precise position measurement is beneficial.

Acknowledgments

A portion of this work was supported by the United States Department of Energy under Contract DE-AC04-94AL85000. Sandia is a multiprogram laboratory operated by Sandia Corporation, a Lockheed Martin Company, for the United States Department of Energy. Additional support was supplied by the Specialty Metals Processing Consortium:

References

1. F. J. Zanner: *Metall. Trans. B*, 1979, 10B, pp. 133-42.
2. F. J. Zanner: *Metall. Trans. B*, 1981, 12B, pp. 721-8;
3. R.L. Williamson, F. J. Zanner, and S.M. Grose: *Metall. And Mater. Trans. B*, 1997, 28B, pp. 841-53.
4. D. K. Melgaard, R. L. Williamson and J. J. Beaman: *JOM*, 1998, vol. 50(3), pp. 13-17.

- 5. Though this paper is focused on electrode gap dynamics and control, it is possible to generalize the treatment to the dynamics of the VAR process as a whole, in which case it is essential to include the melt rate response to melting current.
- 6. The term "measurement" as used here means not only direct measurements but also derivations based on direct measurements. Thus, electrode gap is termed a measured variable even though it must be calculated from drip-short frequency or voltage data.
- 7. See, for example, B. Friedland, *Control System Design, An Introduction to State Space Methods*, McGraw-Hill, Inc., New York, NY, 1986. Also, *Applied Optimal Estimation*, A. Gelb, ed., M.I.T. Press, Cambridge, MA, 1994.